International Journal of Technology v(i) pp-pp (YYYY)
Received Month Year / Revised Month Year / Accepted Month Year

International Journal of Technology

http://ijtech.eng.ui.ac.id

Preparation and Characterization of Activated Carbon from Cavendish Banana (*Musa acuminata*) Peel for Ferric Ions Removal

Put authors name here[1i], Put author name here[1], Put author name here[1], Put author name here[2], Put authors name here[2]

[1]*Put author's affiliation here, complete with address, postal code, and country*
[2]*Put author's affiliation here, complete with address, postal code, and country*

Note: because of double-blind review policy, please only put authors' information (including in header and footer) after accepted at peer review process.

Abstract. This research was conducted to investigate the effect of carbonization temperature, type, and acid concentration as an activating agent on the physicochemical properties of activated carbon made from banana (*Musa acuminata*) peel waste. Carbonization was performed at four different temperatures of 200, 300, 400, and 500°C for two hours, while chemical activation was carried out using varying concentrations of hydrochloric and phosphoric acids. During the experiment, the carbon was impregnated with HCl and H_3PO_4 at three varying solution concentrations of 3, 6, and 9 % for 24 hours. Subsequently, sample characterization was conducted using SNI 06-3730-1995, morphology was observed with SEM, the functional group was analyzed using FT-IR, and the physicochemical properties was observed using BET equipment. The activated carbon was used as an adsorbent to remove ferric ions and iodine (I_2) from the solution. The results showed that the product derived from carbonization at 300°C and activation using 9% hydrochloric acid yielded the highest adsorption capacity of 1.104 mg/g for ferric ions and 1881.51mg/g for iodine. Activated carbon derived from banana peels can be regenerated up to four times, but its efficiency decreases to 75%.

Keywords: Activated carbon; Banana peel; Carbonization; Acid activation; Ferric ions adsorption

1. Introduction

The high population growth and increasing urbanization in the last few decades are associated with heightened water scarcity and low quality. Conventional treatment methods such as disinfection, desalination, and decontamination have been used to solve many water supply quality problems. However, these methods cannot be widely applied due to the expensive costs. The residues produced from the processes also contribute to freshwater contamination (Adekanmi, 2021), underscoring the need to develop new methods. Adsorption is a promising technology due to the simple infrastructure, better efficiency, and effectiveness. Several different adsorbents have been reported for the treatment of polluted water (Basuki et al., 2021; Darmadi et al., 2023; Dhaneswara et al., 2024; Kusrini et al., 2021; Timotius et al., 2022)

[i]Corresponding author's email: name@ai.ue.oa, Tel.: +00-00-000000; Fax: +00-00-000000
doi: 10.14716/ijtech.v0i0.0000

Among the existing adsorbents, activated carbon is considered effective for solving various water problems, from taste and odor to the removal of unwanted contaminants including heavy metals, chlorine, and volatile organic compounds (VOCs)(Basheer et al., 2021; Peláez-Cid et al., 2020; Sanchez-Sanchez et al., 2020; Yu et al., 2020; Zhang et al., 2019). Activated carbon is a material with a very high surface area, prepared with both physical and chemical methods. Physical treatment consists of a two-step process comprising carbonization followed by gasification of oxidizing agents usually CO_2 and water vapor. Meanwhile, chemical treatment is a one-step process where carbonization and activation coincide. Commonly used chemical compounds include $ZnCl_2$, H_3PO_4, KOH, and NaOH (ElShafei et al., 2014; Mistar et al., 2020; Wang and Xu, 2024). The high cost of production has been the most challenging part of commercially producing activated carbon. Therefore, inexpensive raw materials with high carbon, low inorganic content workability, minimum impact on the environment, and storage life have become an exciting research focus in recent decades. In this context, a good precursor should also have a high carbon content. Both treatments can produce a very high specific surface area of activated carbon with the formation of oxidative porosity, with the size distribution and shape depending on the raw material and the process conditions. Renewable sources are the most widely used materials due to the exceptional adsorbent properties (Bhushan et al., 2021; Prakash et al., 2021; Yağmur and Kaya, 2021)

Bananas are a widespread fruit available in many parts of the world, including Indonesia where the peels are easily accessible to make activated carbon without significant cost. The application is widely accepted due to several reasons, including the high content of fiber and organic compounds, namely cellulose, lignin, and pectin. These fibers help form a strong structure and large pores in activated carbon. In addition, the organic components produce activated carbon with various pores, including micro- and meso-, which is necessary as an adsorbent for both organic and inorganic pollutants. Another advantage is that banana peel waste decomposes naturally, rendering the use as activated carbon environmentally friendly. These factors altogether make banana peel an attractive choice for manufacturing activated carbon (Anhwange et al., 2009; Jodiawan et al., 2021; T. Falowo et al., 2021; Tripathy et al., 2021; Wikantika et al., 2022; Yanti et al., 2023). The research was focused on using banana peel waste (*Musa acuminata*) to produce activated carbon. This selection of Cavendish banana was based on the high organic carbon content, such as lignocellulose, reaching 97.5% compared to other types, namely Saba (*Musa paradisiaca var. sapientum*) or King bananas (*Musa paradisiaca*) which only ranged from 90-92% (Anhwange et al., 2009). The conversion of banana peel waste into activated carbon will increase the economic value, reduce waste disposal costs, and provide inexpensive raw materials. Previous research (Din et al., 2017) used an acid impregnation process before carbonization Otherwise, our research uses a carbonization process at the beginning stage to form more and stronger activated carbon pores before being activated using an acid solution. With this process, the activated carbon produced had a greater adsorption capacity. In this research, banana peel waste was previously dried, carbonized, and then activated using an acid solution. The product obtained was tested for the performance as an adsorbent to remove ferric ions in solution.

2. Methods

The method for making activated carbon was in line with the research by (Din et al., 2017) but conducted in the reverse order. It can control the structure and pore size and can help produce activated carbon with high adsorption capacity for specific molecules.

The production of activated carbon from Cavendish banana peels consisted of three stages. The initial stage entailed sample preparation and dehydration processes, followed by carbonization and chemical activation. Activated carbon produced at optimum conditions was used as an adsorbent to adsorb ferric ions from the solution, then the adsorption capacity and model were analyzed.

2.1. Sample Preparation

In this experiment, cavendish banana peels were used as a raw material for producing activated carbon. The starting materials were cut into a size of 2 x 2 cm^2 and dried in an oven at 110 °C for 1 hour. The dried samples were prepared by carbonization and chemical activation. The carbonization process was carried out at 200, 300, 400, and 500°C for 2 hours. Subsequently, carbonized samples were crushed and activated in a 3-9 % (by volume ratio) H_3PO_4 and HCl solution for 24 hours. The activated carbon slurry was then placed into a separating funnel to recover the solid part as activated carbon from the liquid. The sample was washed successively with distilled water and dried at 105 °C for 30 minutes to obtain activated carbon. The schematic diagram for producing activated carbon is illustrated in Figure 1. Moisture, ash content, and absorption capacity were analyzed for iodine and ferric ion solutions.

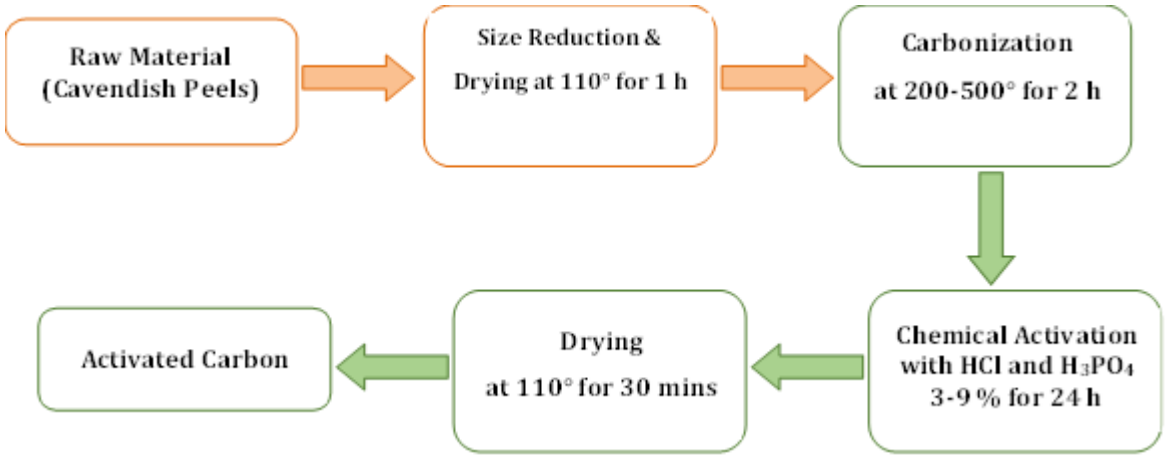

Figure 1. Schematic Diagram for Producing Activated Carbon from Cavendish Banana Peels

2.2. Characterization of Activated Carbon

Activated carbon samples were characterized using SNI 06-3730-1995 standards, including water and ash content analysis and iodine adsorption. Characterization was carried out to measure the quality of the activated carbon produced in several different process conditions.

Table 1. Activated carbon quality based on SNI 06-3730-1995 standards (BSN, 1995)

Parameter	Unit	Requirement
Water content	%	< 15
Ash content	%	< 10
Iodine adsorption	mg/g	>750

Moisture contents were measured by weighing 1 gram of activated carbon, heating at 100 °C for 6 hours, followed by weight measurement.

$$\text{Moisture content (\%)} = \frac{Samples\ mass\ difference}{Initial\ samples\ mass\ before\ heating}\ 100\% \quad (1)$$

Ash contents were measured by combusting 1 g of raw materials in a muffle furnace at 700 ◦ C for 4 hours followed by weighing the activated carbon after heating.

$$\text{Ash content (\%)} = \frac{Total\ ash\ mass}{Initial\ samples\ mass}\ x\ 100\% \quad (2)$$

The iodine number was obtained based on the standard test method (BSN, 1995) by incorporating 0.5 grams of activated carbon into Erlenmeyer containing 25 mL of 0.1 N iodine solution and shaking gently for 15 minutes. The solution was subsequently filtered. The filtrate obtained was placed into an Erlenmeyer and titrated using 0.1 N sodium thiosulphate ($Na_2S_2O_3$) solution until it turned yellowish. About 1 mL of 1% starch solution was added to the solution, and the titration was continued until the solution was clear. The concentration of iodine solution was calculated from a total volume of $Na_2S_2O_3$ used and the volume dilution factor (see equation 3)

$$I = \frac{(V_1N_1 - V_2N_2)x\ Mr\ Iodine\ x\ f_D}{Activated\ carbon\ mass} \quad (3)$$

Where I is Iodine adsorption (mg/g), V_1 is iodine solution volume (mL), N_1 is iodine concentration (N), V_2 is sodium thiosulphate solution volume used (mL), N_2 is sodium thiosulphate concentration (N), Mr is molecular weight (g/mol), and f_D is dilution factor.

The morphological properties of activated carbon was analysed by Scanning Electron Microscopy (SEM). A scanning electron microscope (SEM FEI INSPECT S-50, Netherlands) was used to determine the morphology of the sample. Activated carbon was sprinkled on double-sided carbon tape, placed on the sample holder, and coated with gold.

The FT-IR analysis is utilized to identify the functional groups present in activated carbon. These groups are important for heavy metal adsorption and help to determine the type of adsorption process.heavy metal adsorption and help determine the type of adsorption process. Fourier transform infrared spectroscopy (FTIR Shimadzu IR Tracer 100, Japan) was used to observe functional group changes before and after carbonization using the KBr disc technique. Activated carbon was mixed with dry KBr (ratio of 1:100) and pressed into a transparent disc. FTIR spectroscopy was conducted for the range of 4000 – 400 cm^{-1}. All of the spectra were recorded at room temperature with a resolution of 4 cm^{-1} and 45 scans.

The surface area of a sample was determined using Brunauer-Emmett-Teller (BET) nitrogen adsorption-desorption measurements at 77 K. The Micromeritics Gemini VII Version 5.03 equipment was used to determine the surface area and pore size characteristics through volumetric adsorption of N2 at 77 K. The Activated Carbon was degasified at 300°C for one hour to eliminate any adsorbed species. The nitrogen adsorption at a relative pressure of 0.99 was used to determine the total pore volume.

2.3. Adsorption Model of Ferric ions with Activated Carbon

Using batch experiment, ferric ion solution was mixed with activated carbon and stirred at room temperature. Subsequently, the solutions were filtered, and the ferric ion solution concentrations were determined by Genesys 150 UV-Visible Spectrophotometer (Thermo Scientific, USA) at 510 nm. The equilibrium concentrations of the adsorbates in the solid phase relative to the concentrations in the liquid phase (Q_e, mg/g) of the activated carbon were determined based on adsorbate mass balance using equation (4)(Zhou et al., 2023) :

$$Q_e = \frac{(C_0 - C_e) x\, V}{M} \quad (4)$$

Where Co and Ce are the initial and equilibrium ferric ions concentrations (mg/L), respectively, V is the volume of the aqueous solution (L), and M is the mass of activated carbon used (g).

Adsorption is a process of mass transfer that occurs when material accumulates at the interface between solid and liquid phases. This process is described by equilibrium relationships between sorbent and sorption isotherms, which typically represent the ratio of the quantity of sorbed material to the remaining material in the solution at a fixed temperature and in a state of equilibrium. The adsorption behavior of the activated carbon from Cavendish banana peel waste for ferric ion solution could be elucidated by adsorption models. Many theories have been applied to describe adsorption equilibrium. Numerous isotherm equations are available; however, this study focuses on two key isotherms, namely the Langmuir and Freundlich. The equations for these models are stated as follows (Zhou et al., 2023) :

$$\frac{C_e}{Q_e} = \frac{C_e}{Q_m} + \frac{1}{K_L Q_m} \; (Langmuir) \quad (5)$$

$$ln\, Q_e = ln\, K_f + \frac{1}{n} ln\, C_e \; (Freundlich) \quad (6)$$

Where Q_e, C_0, and C_e are the same as in Eq. (4). Q_m is the maximum theoretical adsorption capacity of activated carbon for ferric ions. K_L and K_F are the adsorption constants of the Langmuir and Freundlich isotherm models related to the adsorption capacity, respectively. 1/n is the constant of adsorption intensity or the surface heterogeneity.

3. Results and Discussion

3.1. Carbonization of Cavendish Banana Peel Waste

Carbonization is an incomplete combustion process of organic material due to limited air availability leading to subsequent decomposition. This process is carried out to produce granular carbon, which has a neat structure, significantly increasing the adsorption ability. A significant decrease in the component of the organic material occurred at 400 °C caused by the decomposition of lignocellulosic biomass, including hemicellulose, cellulose, and lignin. Based on the results, lignin was the first component to decompose at low temperatures and continued up to about 900 °C. At approximately 200 °C, carbonization produced a product similar to biochar and pure carbon.

Hemicellulose decomposed at low temperatures between 200 and 360 °C, while cellulose decomposed at the high-temperature range of 240-390 °C. Furthermore, at 300-400 °C temperature, carbonization tended to produce carbon products with some organic contaminations. At a temperature above 400 °C, the final decomposition of the aromatic lignin fraction occurred, producing carbon purer than the product from the carbonization process at 300-400 °C with insignificant organic contamination (Luangkiattikhun et al., 2008). The characteristics of carbon produced from the carbonization process at different temperatures are listed in Table 2.

Table 2. Carbon characterization after carbonization at different temperatures

Carbonization Temperature, °C	Parameters		
	Moisture Content, %	Ash Content, %	Iodine Adsorption, mg/g
200	30.51	1.80	1845.03
300	28.75	1.32	1881.51
400	29.81	3.22	1855.29
500	30.82	5.57	1728.10

Table 2 shows that the moisture content obtained from the carbonization process at various temperatures ranged from 28.75 - 30.82 %. The lowest moisture content of 28.75 % occurred at a carbonization temperature of 300 °C. Increasing the temperature caused heightened decomposition of all organic components. This led to the production of carbon with more pores and a regular shape. In addition, elevated temperature caused an increase in moisture equilibrium of the carbon material with the environment. The highest moisture content was obtained at a carbonization temperature of 500 °C.

Carbonization at 200 °C produced carbon with a higher moisture content than at 300 °C. This was because most of the lignocellulose, namely hemicellulose and cellulose have not been decomposed at 200 °C. Therefore, the carbon produced had various organic contents, causing an increase in moisture content. Table 2 shows that the carbon ash content was in the range of 1.80 – 5.57 %. Ash is produced from the combustion of organic materials containing mineral and inorganic compounds. The high ash content of carbonized carbon will reduce the performance because the ash potentially causes blockages in the pores and reduces adsorption capability (Sudaryanto et al., 2006; Tongpoothorn et al., 2011). The higher the carbonization temperature used, the greater the ash content value of the activated carbon (Hendrawan et al., 2017). Based on the results, there was an increase in iodine absorption resulting from carbonization at 300˚C. This increase was attributed to higher carbon yield and increased pore volume. The pores formed were also more regular than those of the previous one leading to a larger surface area of the carbon material (Hendrawan et al., 2017). The increased number of pores and the carbon surface area enhanced absorption capacity, thereby improving iodine adsorption. However, carbonization at 400 and 500˚C decreased the absorption capacity for iodine. This was due to the higher amount of moisture and ash content produced compared to carbonization temperature of 300 C. The high ash content led to blockage of the carbon pores and affected iodine adsorption capacity. In addition, the high moisture content also caused the carbon sites to be filled with water molecules, preventing the adsorption of iodine.

3.2. Activation of Carbon Produced of Cavendish Banana Peel Waste

Activation is a process that aims to increase the ability of activated carbon to absorb chemical compounds, gases, or other substances. The process produces a larger surface with more pores to adsorb more compounds. Chemically, carbon is treated with phosphoric acid, sulfuric acid, or alkali metals . The chemicals remove organic materials bound to carbon and open pores. Phosphoric acid was used to activate the carbon and characteristics observed after the activation process are presented in Table 3.

Table 3. The characteristics of activated carbon after activating at different acids and concentrations (Carbonization temperature at 300 °C)

Activator	Parameters		
	Moisture Content, %	**Ash Content, %**	**Iodine Adsorption, mg/g**
3 % H_3PO_4	21.49	2.81	1866.22
6 % H_3PO_4	19.41	3.56	1884.69
9 % H_3PO_4	18.36	2.95	1885.81
3 % HCl	30.35	4.93	1894.53
6 % HCl	27.06	4.41	1899.91
9 % HCl	22.31	3.39	1914.24

Table 3 shows that the moisture content of the activated carbon after acid activation ranged from 19.41 - 30.35 %, with the lowest value obtained using the H_3PO_4 as an activator. The decrease in moisture content was attributed to H_3PO_4(Pujiono et al., 2017), which accelerated the drying process, producing lower moisture content compared to the result of HCl. The higher the activator concentration, the lower the activated carbon moisture content (Hendrawan et al., 2017). Phosphoric acid is generally easier to control in reactions due to the lower acidity. It minimizes the risk of damage or excessive crushing of activated carbon during activation. Furthermore, phosphoric acid is more suitable for applications requiring larger carbon pores and is less acid. Table 3 shows that the ash content of activated carbon after acid activation ranged from 2.81 - 4.93 %.

The range of activator concentrations did not significantly affect the ash content of activated carbon. However, the H_3PO_4 activator produced a lower ash content compared to HCl, which was more effective in removing organic materials from activated carbon. The result was consistent with previous research conducted by (Nurrahman et al., 2021). Increasing acid concentration during activation enhanced the adsorption capacity. Higher acid concentration is associated with a greater possibility of a reaction between the activating agent and activated carbon, producing a more significant amount of both micropores and mesopores (Moreno-Piraján and Giraldo, 2010; Tongpoothorn et al., 2011). The surface area of activated carbon was increased with higher acid concentration, which enhanced the adsorption capacity. The high iodine adsorption capacity indicates the excellent quality of activated carbon (Maulinda, L. et al., 2015).

Table 4. The iodine adsorbed by activated carbon obtained from different carbon sources

Adsorbent	Qe (mg/g) for I_2	Reference
AC banana peel	1914.24	
ACC	1186.17	(Maneechakr and Karnjanakom, 2017)
CB	307.82	
401	380.01	
402	397.98	
501	580.33	
502	590.56	
AC with soaking HF	300	(Buasri A et al., 2013)
AC without soaking HF	290	

Table 4 shows a comparison of the adsorption characteristics of activated carbon on iodine from banana peel sources and other activated carbon sources. These results suggest that activated carbon derived from Cavendish banana peels has a higher iodine adsorption capacity compared to Jatropha curcas waste and other agricultural waste (rice husk, corncob, and wheat straw) (Buasri A et al., 2013; Maneechakr and Karnjanakom, 2017).

3.3. The Morphology of Activated Carbon Prepared from Cavendish Banana Peels

Figure 2a shows carbon from banana peels after carbonization using a furnace at 300 °C for 2 hours. During the carbonization process, the yellow banana peel turned black. The activated carbon morphologies at 1.00 Kx magnifications before and after the activation process are shown in Figures 2b and 2c. Figure 2b shows a rough and compact surface with irregular shape pores. The surface was also microporous with vast heterogeneity. After the activation process, the morphology changed into porous materials of regular shape and opened pores. After the carbonization and acid activation process, tiny pores with a diameter less than 6 μm are formed. Acid activation tends to increase the number and diameter of these pores. Additionally, the presence of 9% acidic chloride results in larger pore size and opening of tinier pores. This indicates that acidic chloride can effectively remove hydrocarbon compounds that may remain attached to the carbon surface after the carbonization process.

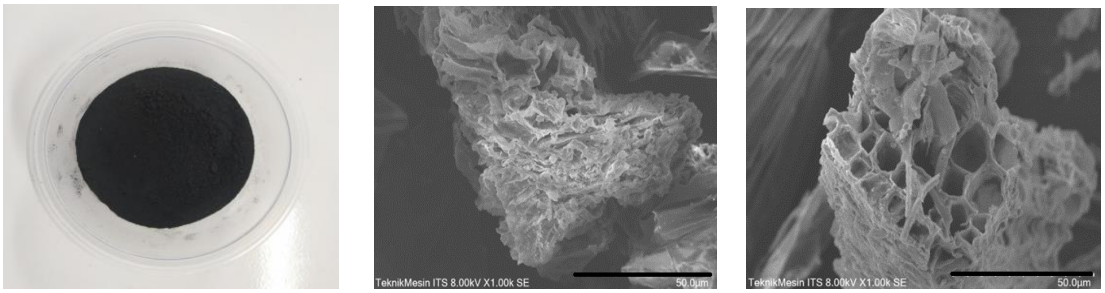

(a) (b) (c)

Figure 2. Producing activated carbon from Cavendish banana: (a) Carbon after carbonization at 300 °C; Scanning Electron Microscopy (SEM) with scale bar 50ɥm of (b) Carbon after carbonization; (c) Carbon after activation

3.4. The FTIR identification of Activated Carbon prepared from Cavendish Banana Peel

Figure 3 displays the FTIR spectra of dried banana peels and activated carbon within the 4000-400 cm^{-1} range.

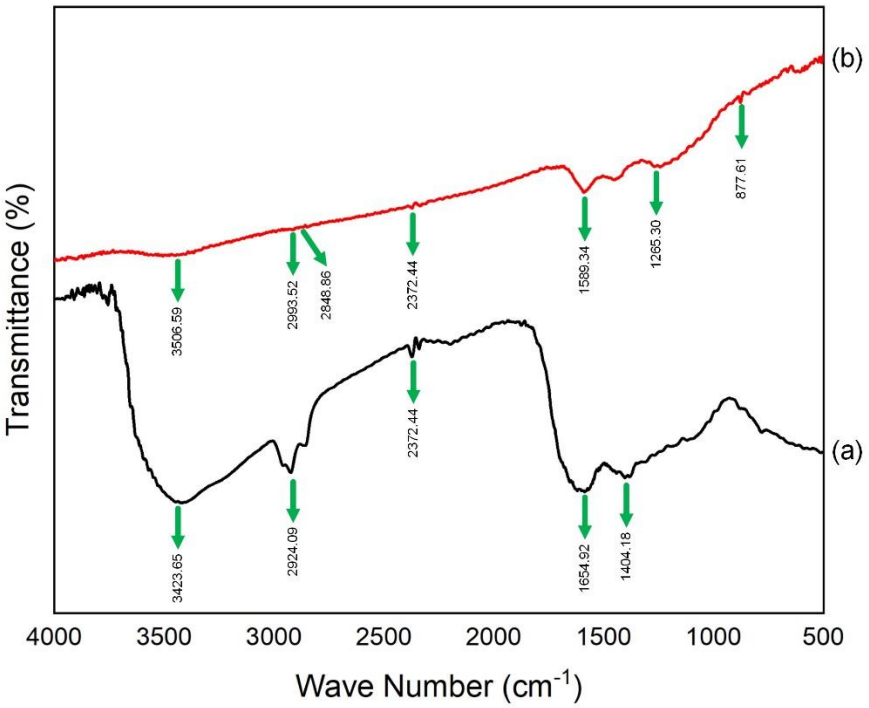

Figure 3. FTIR spectra of (a) dried Banana peels, and (b) activated carbon after carbonization and acid activation

As depicted, the bands in the region of 3423 cm^{-1} indicate the presence of the stretching vibration of amine (–NH) and O-H functional groups (Al-Tabakha et al., 2021) . The band at 2924 cm^{-1} is assigned to aliphatic acids C–H stretching vibrations (Alaa El-Din et al., 2018). The band at 1654 cm^{-1} represents the skeletal aromatic vibrations of C=C in lignin(Gonultas and Candan, 2018), and the band at 1404 cm^{-1} is assigned to –C-H bending. Meanwhile, the results of FT-IR analysis on activated carbon can be seen that this has occurred changes in the infrared (IR) absorption spectrum pattern, namely a reduction in intensity at wave numbers from 3423 cm^{-1}, 2924 cm^{-1}, 2372 cm^{-1}, and 1404 cm^{-1}. Then, new absorptions are formed at wave numbers 2848 cm^{-1}, which is the C-H stretching vibration of methyl (CH_3) and methylene (CH_2) groups, and 1265 cm^{-1} represents the C-O functional group. Carbonization and activation processes have also been established for aromatic C=C bonds at wave number 1589 cm^{-1}. It proved that carbonization and chemical activation had increased the aromatic compounds. These compounds are structural components of hexagonal activated carbon. They show the pore structure of activated carbon and are validated from morphological analysis by SEM. The activated carbon produced has an absorption pattern with OH, C-H, C-O, and C=C bond types. OH and C-O bonds indicate that activated carbon tends to be polar. Thus, the activated carbon produced can be used as an adsorbent for compounds that tend to be polar (Wibowo et al., 2011)

3.5. Brunauer-Emmet-Teller (BET) Analysis

The activated carbon was analyzed using BET equipment to determine its physicochemical properties after being subjected to carbonization and chemical activation. The BET surface area of the activated carbon was found to be 272.84 m^2/g after carbonization and 421.63 m^2/g after activation. The analysis revealed that the activated carbon possessed total pore volumes of 0.217 cm^3/g and 0.319 cm^3/g, and average pore diameters of 3.188 nm and 3.024 nm after carbonization and chemical activation (HCl 9%), respectively. The FTIR results showed that the chemical activation caused the loss of organic compounds in the activated carbon, leading to an increase in surface area and total pore volume. The activated carbon had an average pore size within the mesoporous range (2–50 nm).

Table 5 presents a comparison of the surface area of activated carbon derived from banana peels and other natural materials. The materials were activated through acid impregnation followed by carbonization.

Table 5. Comparison of different adsorbent related to their activated treatments

Raw Materials of Adsorbent	Impregnating Agent	Surface Area S_{BET} (m^2/g)	Reference
Banana peel	HCl	421.63	-
Sun flower oil cake	H_2SO_4	241	(Ratan et al., 2018)
Bamboo	HCl	482	(Mui et al., 2010)
	HNO_3	295	
	H_2SO_4	554	
Carbon	HClO	74-79	(Din et al., 2017)

Based on the data presented in Table 5, the activated carbon produced from banana peels through a carbonization process and then treated with HCl exhibited superior results as compared to the activated carbon obtained from solid waste generated during the production of sunflower oil, which was treated with H_2SO_4. This may be because the fiber structure of banana peel waste is longer than that of sunflower oil cake waste. However, the activated carbon obtained from bamboo demonstrated better results than the activated carbon produced from banana peels through HCl activation. This could be attributed to the compact, long, and sturdy structure of bamboo, which results in the formation of solid pores in the activated carbon.

3.6 Adsorption Performance of Activated Carbon for Ferric Ions Removal

According to the data shown in Figure 4, the process of adsorption can be divided into two stages: a fast and a slow stage. During the initial stage of adsorption (0-45 min), the ferric ions were quickly adsorbed onto the available sites on the surface of the activated carbon. As the adsorption time increased, the adsorption capacity of the activated carbon for ferric ions increased as well, reaching a maximum of 1.1015 mg/g after 90 minutes of adsorption. However, after this point, the number of available adsorption sites on the surface of the activated carbon began to decrease, causing the adsorption capacity to gradually reach saturation. During the slow stage of adsorption (45-90 min), the adsorption capacity of ferric ions increased from 0.7794 mg/g to 1.102

mg/g. This indicates that the adsorption process is time-dependent and that it is important to optimize the adsorption time to achieve the maximum adsorption capacity. (Wang and Xu, 2024)

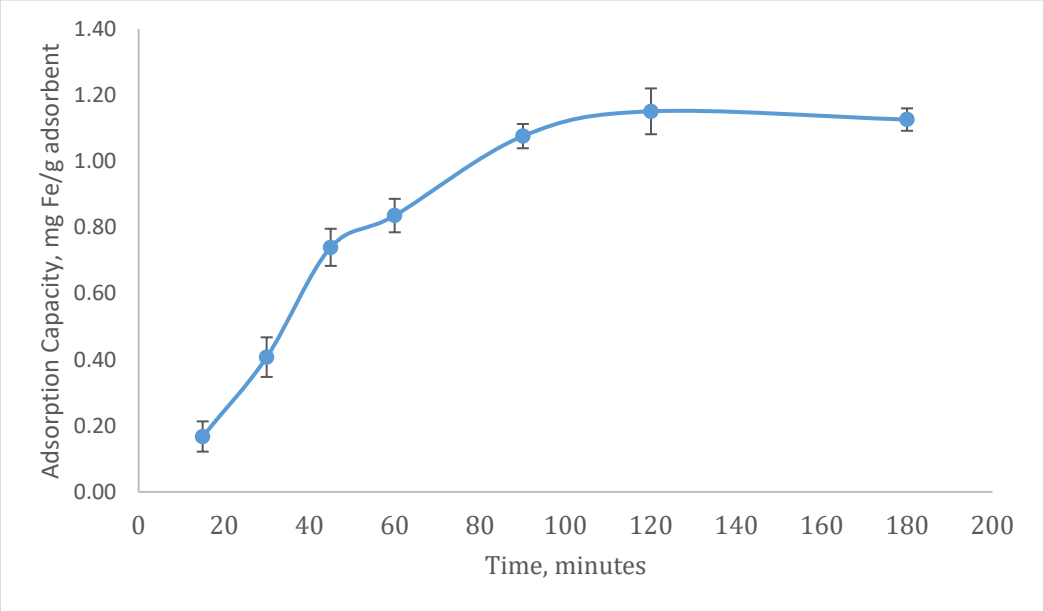

Figure 4. Ferric ions adsorption using activated carbon from Cavendish banana Peels

The initial Fe ions concentration of 2.8 mg/L resulted in an adsorption capacity of 1.1015 mg Fe/g of activated carbon. Activated carbon obtained from banana peels can be regenerated up to four times, but its efficiency reduces to 75% after each regeneration.

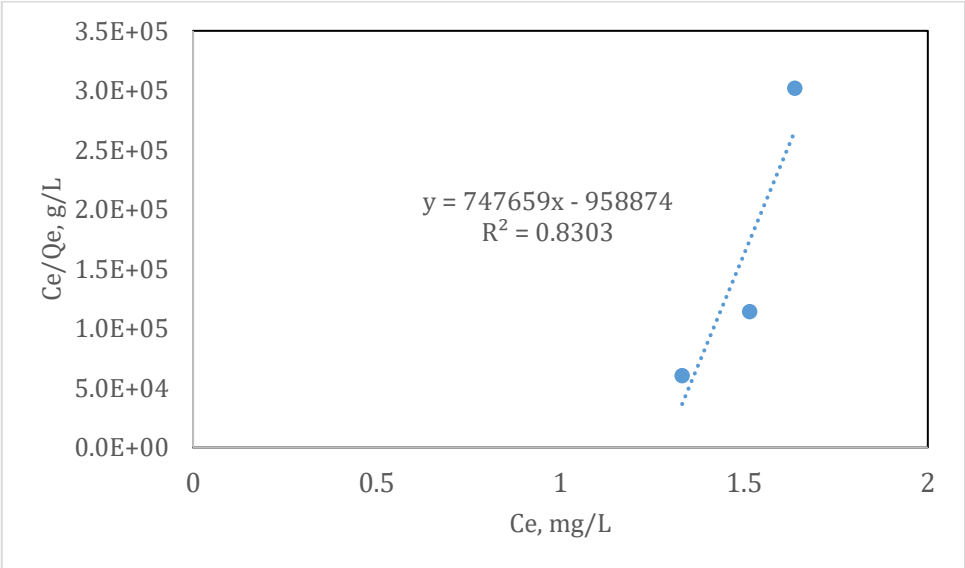

Figure 5. Linear fit of Langmuir isotherm adsorption of ferric ions by activated carbon from Cavendish banana peels

The Freundlich model's correlation coefficient (R^2) is closer to 1 and has a higher value than the Langmuir model. The Freundlich isotherm is based on the assumption that adsorption occurs on sites with non-uniform energy level distribution, rather than on a uniform surface. This means that adsorption is reversible and not limited to monolayer formation. The R^2 values in Figures 5 and 6 suggest that the adsorption of ferric ions in this study is well-suited to the Freundlich model, and that heterolayer ferric ions can form on the adsorbent surface. This phenomenon can be explained by the surface chemistry of banana peel. Banana peel has active functional groups with different intensities and non-uniform distribution, which can affect its adsorption power by causing differences in the energy level of the active sites available on its surface (Achak et al., 2009). Active sites with higher energy levels tend to form heterolayer ferric ions adsorption . This indicates that activated carbon's adsorption of ferric ions is mainly dominated by physical adsorption, such as van der Waals force and Cπ – cation interactions. Van der Waals interactions occur between iron ions and activated carbon due to the uneven distribution of electrons and the resulting dipole moment. Metal ions interact with activated carbon through Cπ-Fe^{3+} interactions, allowing them to adsorb onto its surface and into its pores. Other studies have also shown that the activated carbon system is best represented by the Freundlich model, which has a capacity of 0.027 mg Fe/g activated carbon (Meisrilestari et al., 2013).

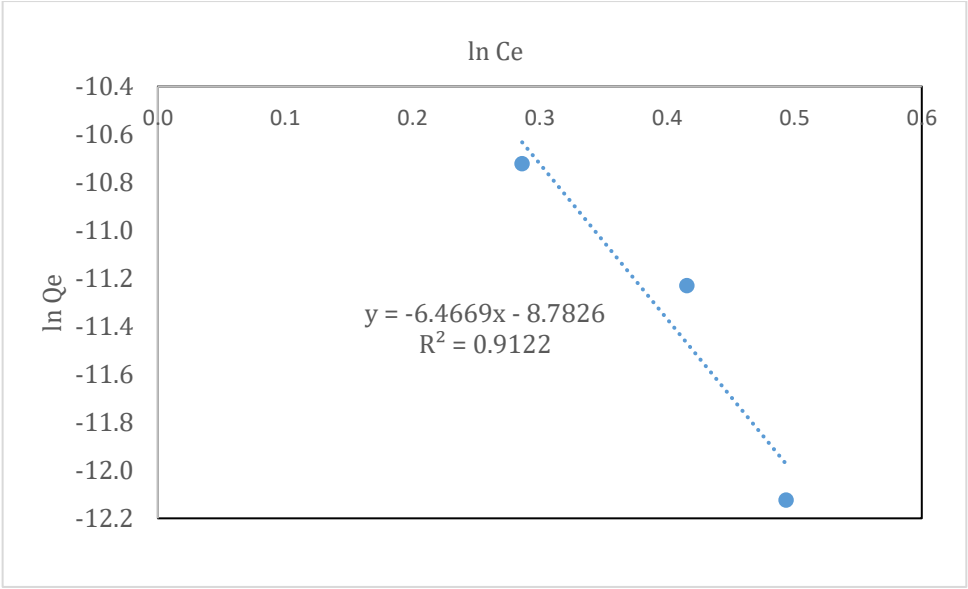

Figure 6. Linear fit of Freundlich isotherm adsorption of ferric ions by activated carbon for Cavendish banana peels

Table 6 The heavy metal adsorbed by activated carbon obtained from different carbon sources

Adsorbent	Qe (mg/g) for Fe^{3+}	Qe (mg/g) for Fe^{2+}	Qe (mg/g) for $Cr_2O_7^{2+}$	Reference
AC banana peel	1.102			
ACC		5.42	0.72	(Maneechakr and Karnjanakom, 2017)
CB		13.53	0	
401		14.55	0	
402		15.80	0	
501		21.33	0	
502		23	0	
AC Betel nut skin		1.4174		(Herlinawati et al., 2023)

Table 6 provides a comparison of the heavy metal adsorption capabilities of activated carbon sourced from banana peels and other agricultural waste. Based on the data presented, it appears that activated carbon obtained from banana peels and betel nut skins have a lower adsorption capacity compared to activated carbon derived from other forms of agricultural waste. This could be due to several factors, including the presence of mesopores in the activated carbon obtained from banana peels, which may not be suitable for Fe^{3+} ions. Moreover, the larger pore size of the activated carbon allows for easier access to Fe^{3+} ions, which can enter the activated carbon structure more readily. Additionally, the pH level during the adsorption test can also affect the adsorption capacity of the activated carbon.

4. Conclusions

In conclusion, Cavendish banana peel waste could be used to effectively prepare activated carbon. Based on the results, the suitable conditions to achieve optimum iodine number were 300**°C** carbonization temperature, 24-hour activation time, and 9% hydrochloric acid. The adsorption capacity for iodin and ferric ions reached 1914.24 and 1.1015 mg Fe/g activated carbon and fit the Freundlich isotherm model. Activated carbon obtained from banana peels can be regenerated up to four times, but its efficiency reduces to 75% after each regeneration.

Acknowledgments

The author acknowledges financial support from the Indonesian Ministry of Research, Technology, and Higher Education through the Basic Research Scheme for Higher Education Excellence under contract numbers 077/E5/PG.02.00.PL/2023 and 004/SP2H/PT-L/LL7/2023..

References

Achak, M., Hafidi, A., Ouazzani, N., Sayadi, S., Mandi, L., 2009. Low cost biosorbent "banana peel" for the removal of phenolic compounds from olive mill wastewater: Kinetic and equilibrium studies. J Hazard Mater 166, 117–125. https://doi.org/10.1016/j.jhazmat.2008.11.036

Adekanmi, A.T., 2021a. Health Hazards of Toxic and Essential Heavy Metals from the Poultry Waste on Human and Aquatic Organisms, in: Patra, A.K. (Ed.), Animal Feed Science and Nutrition. IntechOpen, Rijeka. https://doi.org/10.5772/intechopen.99549

Alaa El-Din, G., Amer, A.A., Malsh, G., Hussein, M., 2018. Study on the use of banana peels for oil spill removal. Alexandria Engineering Journal 57, 2061–2068. https://doi.org/https://doi.org/10.1016/j.aej.2017.05.020

Al-Tabakha, M.M., Khan, S.A., Ashames, A., Ullah, H., Ullah, K., Murtaza, G., Hassan, N., 2021. Synthesis, characterization and safety evaluation of sericin-based hydrogels for controlled delivery of acyclovir. Pharmaceuticals 14. https://doi.org/10.3390/ph14030234

Anhwange, B., Ugye, J., Nyiatagher, T.D., 2009. Chemical Composition of Musa sepientum (Banana) Peels. Electronic Journal of Environment, Agriculture and Food Chemistry 8, 437–4442.

Basheer, A.O., Hanafiah, M.M., Alsaadi, M.A., Al-Douri, Y., Al-Raad, A.A., 2021. Synthesis and optimization of high surface area mesoporous date palm fiber-based nanostructured powder activated carbon for aluminum removal. Chin J Chem Eng 32, 472–484. https://doi.org/10.1016/j.cjche.2020.09.071

Basuki, K.T., Fatuzzahroh, M., Ariyanti, D., Saputra, A., 2021. Adsorption of Strontium from an Aqueous Solution by TiO2-Pillared Zeolite. International Journal of Technology 12, 625–634. https://doi.org/10.14716/ijtech.v12i3.4376

Bhushan, B., Nayak, A., Kotnala, S., 2021. Green synthesis of highly porous activated carbon from jackfruit peel: Effect of operating factors on its physico-chemical characteristics. Mater Today Proc 44, 187–191. https://doi.org/10.1016/j.matpr.2020.08.554

BSN, 1995, SNI 06-3730-1995 Arang Aktif Teknis

Buasri A, Chaiyut N, Loryuenyong V, Phakdeepatraraphan E, 2013. synthesis-of-activated-carbon-using-agricultural-wastes-from-biodiesel-production. International Journal of Materials and Metallurgical Engineering 7, 106–110.

Darmadi, Lubis, M.R., Masrura, M., Syahfatra, A., Mahidin, 2023. Clay and Zeolite-Clay Based Monoliths as Adsorbents for the Hg(II) Removal from the Aqueous Solutions. International Journal of Technology 14, 129–141. https://doi.org/10.14716/ijtech.v14i1.5134

Dhaneswara, D., Tsania, A., Fatriansyah, J.F., Federico, A., Ulfiati, R., Muslih, R., Mastuli, M.S., 2024. Synthesis of Mesoporous Silica from Sugarcane Bagasse as Adsorbent for Colorants Using Cationic and Non-Ionic Surfactants. International Journal of Technology 15, 373. https://doi.org/10.14716/ijtech.v15i2.6721

Din, M.I., Ashraf, S., Intisar, A., 2017. Comparative study of different activation treatments for the preparation of activated carbon: A mini-review. Sci Prog. https://doi.org/10.3184/003685017X14967570531606

ElShafei, G.M.S., ElSherbiny, I.M.A., Darwish, A.S., Philip, C.A., 2014. Silkworms' feces-based activated carbons as cheap adsorbents for removal of cadmium and methylene blue from aqueous solutions. Chemical Engineering Research and Design 92, 461–470. https://doi.org/https://doi.org/10.1016/j.cherd.2013.09.004

Gonultas, O., Candan, Z., 2018. Chemical characterization and ftir spectroscopy of thermally compressed eucalyptus wood panels. Maderas: Ciencia y Tecnologia 20, 431–442. https://doi.org/10.4067/S0718-221X2018005031301

Hendrawan, Y., Sutan, S.M., Kreative, R., Keteknikan, J., Teknologi, P.-F., Brawijaya, P.-U., Malang, J.V., 2017. Pengaruh Variasi Suhu Karbonisasi dan Konsentrasi Aktivator terhadap Karakteristik Karbon Aktif dari Ampas Tebu (Bagasse) Menggunakan Activating Agent NaCl (*The effect of different carbonization temperatures and activator concentrations on the characteristics of activated carbon from bagasse using NaCl as an activating agent*), Jurnal Keteknikan Pertanian Tropis dan Biosistem.

Herlinawati, H., Layla Sihombing, J., Kembaren, A., Simatupang, L., Adhani, R., 2023. Analysis of Fe metal adsorption in industrial wastewater using adsorbents from betel nut skin. Jurnal Pendidikan Kimia 15, 35–40. https://doi.org/10.24114/jpkim.v15i1.42478

Jodiawan, Chrisdiyanti, D.N., Vi'atin, N., Prihastyanti, M.N.U., Chandra, R.D., Heriyanto, Siswanti, C.A., Hapsari, L., Brotosudarmo, T.H.P., 2021. Carotenoid analysis from commercial banana cultivars (Musa spp.) in malang, east java, indonesia. Indonesian Journal of Chemistry 21, 690–698. https://doi.org/10.22146/ijc.60865

Maulinda, L., Nasrul, Z.A., Sari, D.N., 2015. Pemanfaatan Kulit Singkong Sebagai Bahan Baku Karbon Aktif (*Utilization of Cassava Peel as Raw Material for Active Carbon*), Jurnal Teknologi Kimia Unimal, Jurnal Teknologi Kimia Unimal.

Kusrini, E., Ayuningtyas, K., Mawarni, D.P., Wilson, L.D., Sufyan, M., Rahman, A., Prasetyanto, Y.E.A., Usman, A., 2021. Micro-structured Materials for the Removal of Heavy Metals using a Natural Polymer Composite. International Journal of Technology 12, 275–286. https://doi.org/10.14716/ijtech.v12i2.4578

Luangkiattikhun, P., Tangsathitkulchai, C., Tangsathitkulchai, M., 2008. Non-isothermal thermogravimetric analysis of oil-palm solid wastes. Bioresour Technol 99, 986–997. https://doi.org/10.1016/j.biortech.2007.03.001

Maneechakr, P., Karnjanakom, S., 2017. Adsorption behaviour of Fe(II) and Cr(VI) on activated carbon: Surface chemistry, isotherm, kinetic and thermodynamic studies. J Chem Thermodyn 106, 104–112. https://doi.org/https://doi.org/10.1016/j.jct.2016.11.021

Meisrilestari, Y., Khomaini, R., Wijayanti, H., 2013. Pembuatan Arang Aktif dari Cangkang Kelapa Sawit dengan Aktivasi secara Fisika, Kimia dan Fisika-Kimia (*How to make activated charcoal from palm oil shells using physical, chemical, and physical-chemical activation methods*). Konversi 2, 45. https://doi.org/10.20527/k.v2i1.136

Mistar, E.M., Alfatah, T., Supardan, M.D., 2020. Synthesis and characterization of activated carbon from Bambusa vulgaris striata using two-step KOH activation. Journal of Materials Research and Technology 9, 6278–6286. https://doi.org/10.1016/j.jmrt.2020.03.041

Moreno-Piraján, J.C., Giraldo, L., 2010. Study of activated carbons by pyrolysis of cassava peel in the presence of chloride zinc. J Anal Appl Pyrolysis 87, 288–290. https://doi.org/10.1016/j.jaap.2009.12.003

Mui, E.L.K., Cheung, W.H., Cheung, W.H., Valix, M., Mckay, G., 2010. Dye adsorption onto char from bamboo. J Hazard Mater 177 1–3, 1001–5.

Nurrahman, A., Permana, E., Gusti, D.R., Lestari, I., 2021. Pengaruh Konsentrasi Aktivator Terhadap Kualitas Karbon Aktif dari Batubara Lignit. Jurnal Daur Lingkungan 4, 44. https://doi.org/10.33087/daurling.v4i2.86

Peláez-Cid, A.A., Romero-Hernández, V., Herrera-González, A.M., Bautista-Hernández, A., Coreño-Alonso, O., 2020. Synthesis of activated carbons from black sapote seeds, characterization and application in the elimination of heavy metals and textile dyes. Chin J Chem Eng 28, 613–623. https://doi.org/10.1016/j.cjche.2019.04.021

Pujiono, E.F., Mulyati, A., 2017. Potential of Activated Carbon Produced from Agriculture Waste for Water Treatment Material. Institut Ilmu Kesehatan Bhakti Wiyata Kediri

Prakash, M.O., Raghavendra, G., Ojha, S., Panchal, M., Kumar, D., 2021. Investigation of tribological properties of biomass developed porous nano activated carbon composites. Wear 466–467, 203523. https://doi.org/10.1016/j.wear.2020.203523

Ratan, J.K., Kaur, M., Adiraju, B., 2018. Synthesis of activated carbon from agricultural waste using a simple method: Characterization, parametric and isotherms study. Mater Today Proc 5, 3334–3345. https://doi.org/https://doi.org/10.1016/j.matpr.2017.11.576

Sanchez-Sanchez, A., Izquierdo, M.T., Mathieu, S., Medjahdi, G., Fierro, V., Celzard, A., 2020. Activated carbon xerogels derived from phenolic oil: Basic catalysis synthesis and electrochemical performances. Fuel Processing Technology 205, 106427. https://doi.org/10.1016/j.fuproc.2020.106427

Sudaryanto, Y., Hartono, S.B., Irawaty, W., Hindarso, H., Ismadji, S., 2006. High surface area activated carbon prepared from cassava peel by chemical activation. Bioresour Technol 97, 734–739. https://doi.org/https://doi.org/10.1016/j.biortech.2005.04.029

T. Falowo, T., P. Ejidike, I., Lajide, L., S. Clayton, H., 2021. Polyphenolic Content of Musa Acuminata and Musa Paradisiaca bracts: Chemical Composition, Antioxidant and Antimicrobial Potentials. Biomedical and Pharmacology Journal 14, 1767–1780. https://doi.org/10.13005/bpj/2276

Timotius, D., Kusumastuti, Y., Omar, R., Harun, R., Kamal, S.M.M., Jenie, S.N.A., Petrus, H.T.B.M., 2022. The Study of Methylene Blue Loading into Chitosan-graft-Maleic Sponges. International Journal of Technology 13, 1796–1805. https://doi.org/10.14716/ijtech.v13i8.6133

Tongpoothorn, W., Sriuttha, M., Homchan, P., Chanthai, S., Ruangviriyachai, C., 2011. Preparation of activated carbon derived from Jatropha curcas fruit shell by simple thermo-chemical activation and characterization of their physico-chemical properties. Chemical Engineering Research and Design 89, 335–340. https://doi.org/https://doi.org/10.1016/j.cherd.2010.06.012

Tripathy, A., Mohanty, S., Nayak, S.K., Ramadoss, A., 2021. Renewable banana-peel-derived activated carbon as an inexpensive and efficient electrode material showing fascinating supercapacitive performance. J Environ Chem Eng 9, 106398. https://doi.org/https://doi.org/10.1016/j.jece.2021.106398

Wang, K., Xu, S., 2024. Preparation of High Specific Surface Area Activated Carbon from Petroleum Coke by KOH Activation in a Rotary Kiln. Processes 12. https://doi.org/10.3390/pr12020241

Wibowo, S., Syafi, W., Gustan Pari, Nauli, B.A, 2011. Karakterisasi Permukaan Arang Aktif Tempurung Biji Nyamplung (*Surface Analysis of Activated Charcoal from Nyamplung Seed Shells*).Kehutanan Terpadu

Wikantika, K., Ghazali, M.F., Dwivany, F.M., Novianti, C., Yayusman, L.F., Sutanto, A., 2022. Integrated Studies of Banana on Remote Sensing, Biogeography, and Biodiversity: An Indonesian Perspective. Diversity (Basel) 14. https://doi.org/10.3390/d14040277

Yağmur, H.K., Kaya, İ., 2021. Synthesis and characterization of magnetic ZnCl2-activated carbon produced from coconut shell for the adsorption of methylene blue. J Mol Struct 1232. https://doi.org/10.1016/j.molstruc.2021.130071

Yanti, I., Sationo, P.P., Winata, W.F., Anugrahwati, M., Anas, A.K., Swasono, Y.A., 2023. Effectiveness of activated carbon magnetic composite from banana peel (Musa acuminata) for recovering iron metal ions. Case Studies in Chemical and Environmental Engineering 8, 100378. https://doi.org/https://doi.org/10.1016/j.cscee.2023.100378

Yu, F., Zhu, X., Jin, W., Fan, J., Clark, J.H., Zhang, S., 2020. Optimized synthesis of granular fuel and granular activated carbon from sawdust hydrochar without binder. J Clean Prod 276, 122711. https://doi.org/https://doi.org/10.1016/j.jclepro.2020.122711

Zhang, D., He, C., Zhao, J., Wang, J., Li, K., 2019. Facile synthesis of hierarchical mesopore-rich activated carbon with excellent capacitive performance. J Colloid Interface Sci 546, 101–112. https://doi.org/10.1016/j.jcis.2019.03.059

Zhou, P., Li, X., Zhou, J., Peng, Z., Shen, L., Li, W., 2023. Insights of the adsorption mechanism of methylene blue on biochar from phytoextraction residues of Citrus aurantium L.: Adsorption model and DFT calculations. J Environ Chem Eng 11. https://doi.org/10.1016/j.jece.2023.110496